(Received 1 April 2024, Accepted 27 May 2024, Scheduled 10 June 2024)

Design of Wider Impedance Bandwidth with Dual-Port CPW-Fed Slotted Patch Antenna for Wireless Communications

Prudhvi Raj Govathoti, Chirukuri Naga Phaneendra, and Ketavath Kumar Naik*

Antenna Research Laboratory, Department of Electronics and Communication Engineering
Koneru Lakshmaiah Education Foundation (KLEF) deemed to be University, Vaddeswaram, Guntur 522502, India

ABSTRACT: A novel dual-port co-planar wave-guide (CPW)-fed rectangular patch (CRSP) antenna with L-shape and rectangular-shaped slots is proposed for wider impedance bandwidth for wireless communications applications. The dimensions of the overall proposed patch antenna are compact, with a size of $20 \times 40 \times 0.07\,\text{mm}^3$. It operates from 14.6 GHz to 17.4 GHz with an impedance bandwidth of 2.8 GHz. The isolation between elements is greater than 15 dB within the band. A peak gain of 6.74 dBi and a reflection coefficient of -30 dB at operating frequency have been observed. The two-port (multiple-input and multiple-output) CPW-fed antenna parameters like envelope correlation coefficient (ECC), diversity gain (DG), total active reflection coefficient (TARC), channel capacity loss (CCL), and mean effective gain (MEG) are investigated. The simulated and measured characteristics are found to be satisfactory for CRSP antenna model utilized for wireless communication applications.

1. INTRODUCTION

Nowadays, wireless communication systems are an integral part of everyday life. Wider band antennas with low power, reliable systems, high data rates, and fast communication systems have been playing a very significant role. These wide-band antennas are mainly used in military radio, smart metering, fixed satellite communication, mobile communication, and space research applications. To increase wireless data transfer rates and be compatible with the most recent and growing needs, engineers are developing advanced antenna technologies. Many strategies have been offered to support large data rates. Mobile and satellite applications for wireless communication systems now use multiple-input multiple-output (MIMO) technology. The next-generation wireless communication technology, or 5G, has gained a lot of appeal since it can support incredibly high data speeds and has enhanced reliability without using more frequency or bandwidth. At both ends, many antenna elements and ports are used. Moreover, without the requirement for additional radio frequency spectrum, channel capacity increases with the use of MIMO antenna systems. It can be difficult to combine many antennas with the desired level of isolation when MIMO antennas are involved. From the literature survey, to improve the isolation in the MIMO systems, different techniques are used, like ground defective structures, split ring resonators, slots on the ground plane, EBG (electronic band gap) structures, and parasitic strips. From the literature survey, various types of MIMO antenna models with different techniques were used to design antennas for wireless and Ku-band applications. In [1], a compact tri-band rectangular patch antenna is designed for wireless applications. Due to the greater number of defected ground structure (DGS) slots used in the design, complexity increases. Similarly, for Ku band and wireless communication applications [2], a low-profile patch antenna is designed. A CPW-fed E-shaped patch antenna is proposed [3] for X-band applications. However, it is also used for wireless applications. The feeding technique plays a very important role in communication. In [4, 5], CPW-fed antennas for wireless applications are discussed. However, the design dimensions are increased due to its structure.

In past research, the researchers focused more on slots and slits because of their benefits and applications. Triangular and rectangular slots on rectangular patches, along with defective ground structures [6–8], are designed for Ku band and wireless applications. In [9], cylindrical dielectric resonators are used for wide-band wireless applications. The MIMO functional characteristics of the design are not presented due to its low isolation. In [10], a spidroin structure is used for Ku band and wireless applications. A compact quad-port MIMO-antenna has been designed with a rhombus shape for wireless applications [11]. T, U, and tapered-shaped slots on the patch are used for X band, Ku band, and wireless communication applications [12–14]. Wide-band rectangular patch antennas are designed [15, 16] for multi-band applications like X, K, and Ku bands and wireless communication. The CPW feeding technique [17] is used to enhance the isolation of antennas for mobile terminal wireless applications. L-shaped slots on rectangular patches are used for wireless applications [18]. Different guided mode technical characteristics, like Common Mode (CM) and Differential Mode (DM) analysis, are described in the previous literature [19]. In [20, 21], different isolation structures are used to design MIMO antennas for wide-band wireless applications. Because antenna elements are placed orthogonally, the isolation between the antennas is improved.

* Corresponding author: Ketavath Kumar Naik (drkumarkn@hotmail.com).

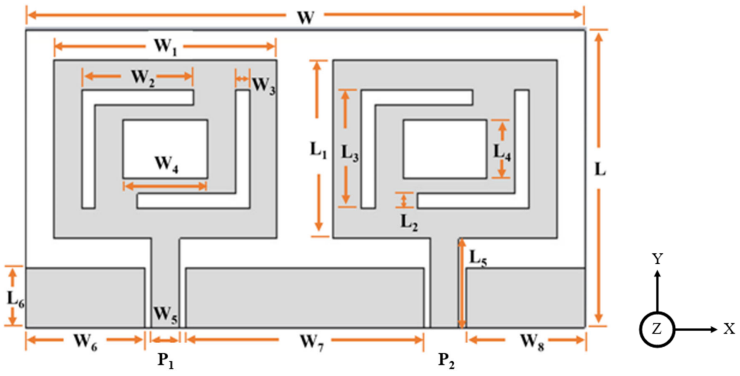

FIGURE 1. Physical structure of CRSP antenna model.

TABLE 1. The parameters of CRSP antenna.

Parameters	Value (mm)	Parameters	Value (mm)	Parameters	Value (mm)
L	20	L_6	4	W_3	1
L_1	12	H_1	0.07	W_4	6
L_2	1	H_2	0.01	W_5	2
L_3	8	W	40	W_6	8.5
L_4	4	W_1	16	W_7	17
L_5	6	W_2	8	W_8	8.5

In [22, 23], an antenna with a CSRR loaded on the patch is made for wireless applications. The MIMO antenna achieves broad impedance bandwidth and strong isolation of more than 20 dB in combination with a decoupling capacitive feeding mechanism [24, 25]. In [26, 27], a compact MIMO antenna system is attained by eight ports with -10 dB isolation within the band. Sub-6 GHz is allotted for the 5th generation table for different countries located there. To know the correlation between MIMO elements, genetic algorithm-based MIMO antennas are designed [28]. In [29], conformal antenna arrays are optimized using a search group algorithm. A circular slot on a meander line antenna is designed [30]. The mean effective gain of the proposed antenna can be obtained from [31, 32] S-parameters.

In this paper, a dual-port single-band CPW-fed rectangle-shaped patch (CRSP) antenna with two L slots and one rectangle-shaped slot along with a partial ground plane is designed for wireless applications. Operating at 16.0 GHz, the proposed antenna produces a bandwidth of 14.6 GHz to 17.4 GHz. The horizontal rectangular slot added to the vertical rectangular slot to form an L-shape slot over the patch is considered for bandwidth enhancement, and the center rectangular slot is considered for enhancing the reflection coefficient, respectively.

2. ANTENNA STRUCTURE

A dual-port CPW-fed rectangular-shaped patch (CRSP) antenna with L and rectangular slots is etched on dual patches for wireless communication applications. Also, the physical structure of the proposed MIMO antenna, i.e., dual-port antenna model is depicted in Fig. 1. Kapton polyimide is considered a substrate material with a height of 0.07 mm and is represented as H_1. The dimensions of the substrate are length (L) and width (W), respectively. The two rectangular patches are placed side by side and considered as port-1 (P_1) and port-2 (P_2) as shown in Fig. 1, with the dimensions of L_1 and W_1 coated on substrate material with a 0.01-mm thickness, which is represented as H_2. The CRSP antenna has a microstrip feed line with an impedance of 50 Ω which is the input to the radiating patch through a rectangular stub with a length and width of L_5 and W_5, respectively, as shown in Fig. 1. There are different parameters used to perform the analysis, and the list of parameters is represented in Table 1.

The length and width of the patch obtained from [33] determine the resonant frequency of the antenna, and the width of the microstrip patch W is given by Equation (1).

$$W = \frac{C}{2f_r}\sqrt{\frac{2}{\varepsilon_r + 1}} \tag{1}$$

where ε_r is the relative dielectric constant, and f_r is the resonant frequency.

The effective dielectric constant, ε_{re}, is calculated as:

$$\varepsilon_{re} = \frac{\varepsilon_r + 1}{2} + \frac{\varepsilon_r - 1}{2}\left[\left(1 + \frac{12t}{W}\right)^{-\frac{1}{2}} + 0.04\left(1 - \frac{W}{t}\right)^2\right] \tag{2}$$

The length of microstrip patch L is given by:

$$L = \left\{\frac{C}{2f_r\sqrt{\varepsilon_{re}}}\right\} \tag{3}$$

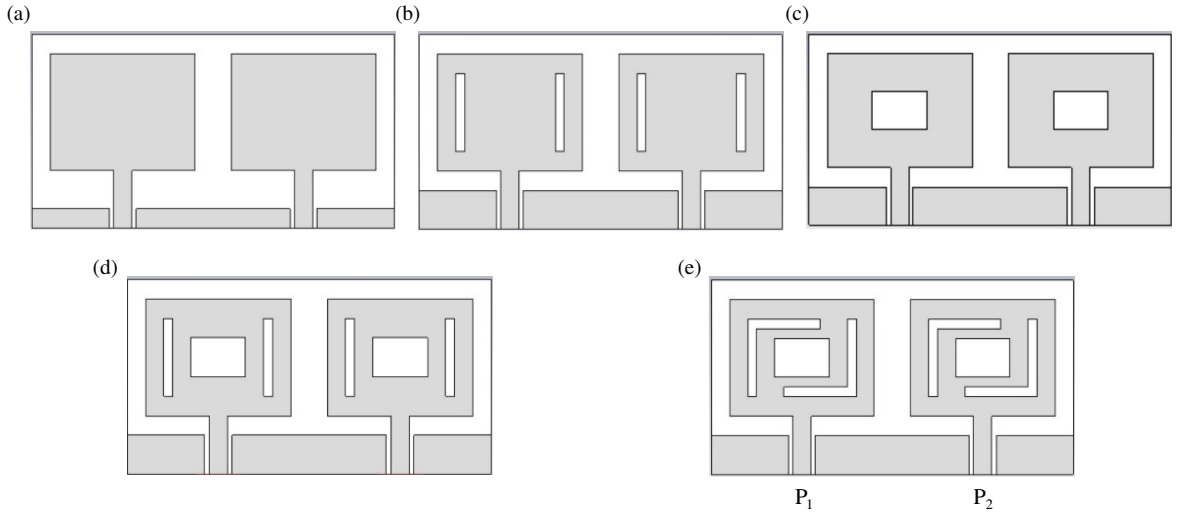

FIGURE 2. Evaluation process of CRSP antenna, (a) Ant. 1, (b) Ant. 2, (c) Ant. 3, (d) Ant. 4, (e) Ant. 5.

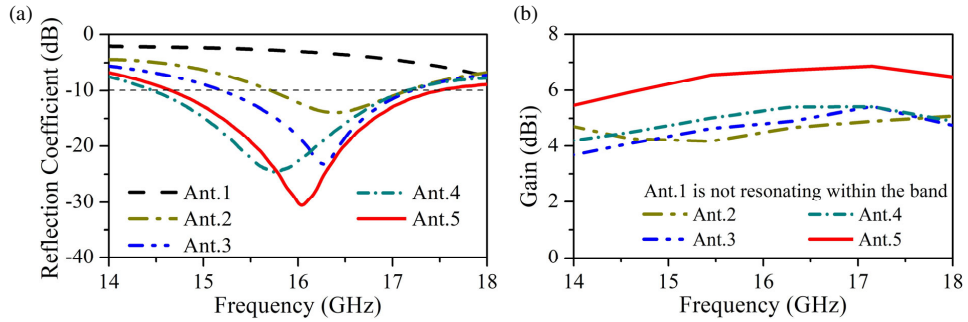

FIGURE 3. Evaluation process of the CRSP antenna, (a) reflection coefficient, (b) gain.

Coplanar Waveguide (CPW) feeding is employed by the proposed antenna. The CPW-feed is considered with length and width L_6 and W_6 and a thickness of 0.01 mm. The two L-shaped slots of opposite directions are embedded on each rectangular radiating patch of the proposed antenna with the dimensions of $L_2 \times W_2$ and $L_3 \times W_3$, along with which another rectangular slot is integrated over the rectangular patch with the dimensions of L_4 and W_4 depicted in Fig. 1.

3. DESIGN PROCEDURE AND ANALYSIS

3.1. Design Process of CRSP Antenna

The detailed evaluation process of the CRSP antenna is shown in Fig. 2. The evaluation process consists of a total of five steps. In all five steps, the coplanar waveguide feeding techniques are used. In the first step of design, dual port plain rectangular patches with a CPW-feed of length 2 mm act as Ant-1 shown in Fig. 2(a). In the second step, the antenna is designed by considering the CPW-fed length 4 mm, and two vertical rectangular slots are embedded with dimensions of $L_3 \times W_3$ as depicted in Fig. 2(b). Ant-2 resonates at 16.3 GHz with a minimum reflection coefficient -13 dB, bandwidth 1.5 GHz, and gain 4.5 dBi.

After that, in the third step, the center rectangular slot is etched from the patch with the CPW-feed to act as Ant-3, as shown in Fig. 2(c). Ant-3 resonates at 16.2 GHz with a reflection coefficient, bandwidth, and gain of -23 dB, 1.9 GHz, and 4.86 dBi. All the antenna parameters are enhanced compared to Ant-2. However, for further enhancement of antenna characteristics, Ant-4 is considered a combination of Ant-2 and Ant-3, as shown in Fig. 2(d). Ant-4 resonates at 15.7 GHz, whose reflection coefficient, bandwidth, and gain are -24 dB, 2.7 GHz, and 5.39 dBi, respectively. Further enhancement of the gain and reflection coefficients happens when we consider Ant-5. Therefore, in the final step, Ant-5 is considered with two L-shaped slots and one rectangular slot on both side patches [considered as port-1 (P_1) and port-2 (P_2)] with the CPW-feed shown in Fig. 2(e). Ant-5 resonates at 16 GHz, whose reflection coefficient, bandwidth, and gain are -30 dB, 2.8 GHz, and 6.74 dBi, respectively. Gain and reflection coefficients are significantly improved. Hence, Ant-5 is considered the CRSP antenna for wireless communication applications.

The CRSP antenna is excited at port-1 (P_1) and port-2 (P_2), with 50-ohm line impedance matching. The separation from center to center of the patches is 20 mm to enhance the isolation between the patches. The proposed model produces better isolation (< -15 dB) between the two patches. The working conditions of the CRSP antenna are considered, when port 1 is excited and port 2 terminated with a matching stub. Similarly, when port 2 is excited, port 1 is terminated with a matching stub. In Figs. 3(a) and (b), the evaluation process steps with re-

TABLE 2. Evaluation process of CRSP antenna model values.

Iteration	Operating frequency (GHz)	Operating Band (GHz)	Gain (dBi)	Reflection Coefficient (dB)
Ant. 1	-	-	-	-
Ant. 2	16.3	15.7–17.2	4.50	−13
Ant. 3	16.2	15.3–17.2	4.86	−23
Ant. 4	15.7	14.5–17.2	5.39	−24
Ant. 5	16.0	14.6–17.4	6.74	−30

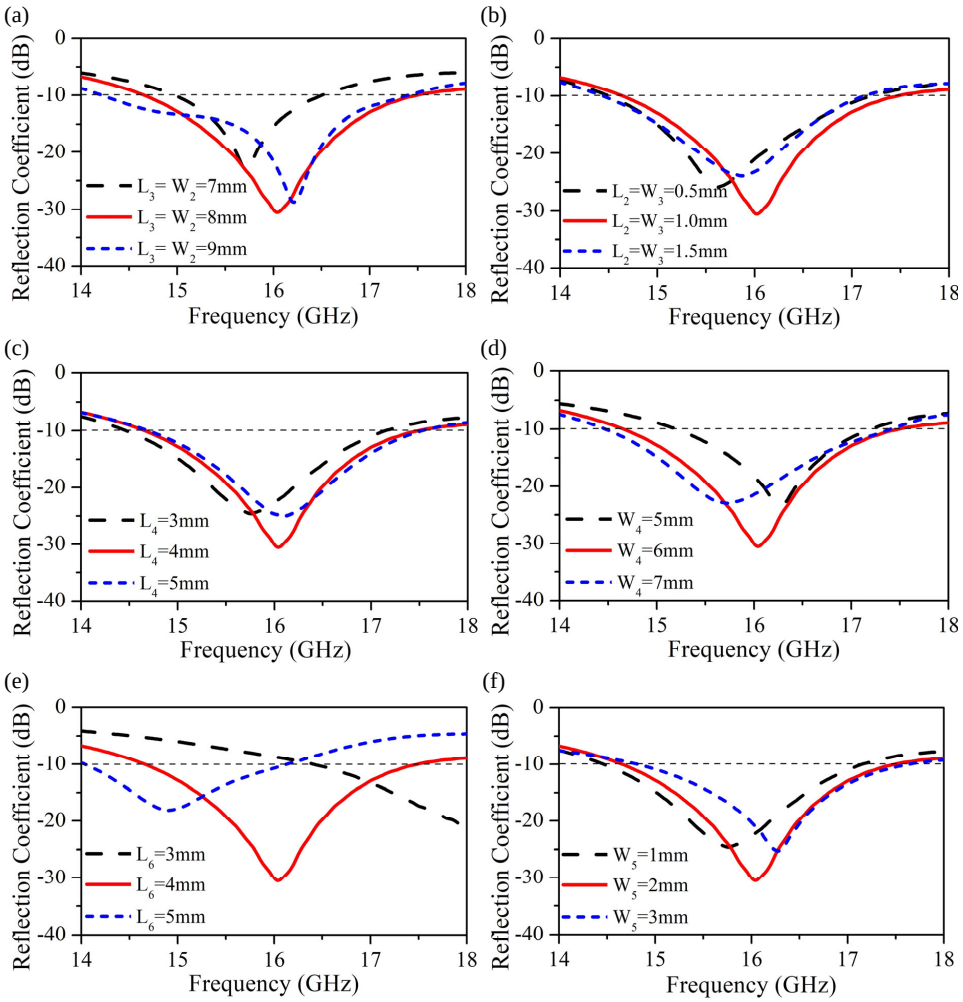

FIGURE 4. Analysis of CRSP antenna parameters, (a) parameter L_3, (b) parameter W_3, (c) parameter L_4, (d) parameter W_4, (e) parameter L_6, (f) parameter W_5.

spect to reflection coefficient and gain are presented. In Table 2, the quantitative analysis of the evaluation method is explained by considering operating frequency (GHz), bandwidth (GHz), gain (dBi), and reflection coefficient (dB).

3.2. Parametric Analysis

Parametric analysis helps to understand the impact of design parameters on antenna performance. A total of 18 parameters are used in the antenna design process, and all these parameters are analyzed. However, out of 18 major parameters, six are displayed in Fig. 4 for brevity. For parametric analysis, antenna performance metrics such as bandwidth, reflection coefficient, and gain are mainly concerned. The parameters $L_3 \times W_2$ and $L_2 \times W_3$ are the dimensions of the L-shaped slots used on the patch. Another important parameter, $L_4 \times W_4$, is also analyzed. These parameters are related to the center rectangular slot on the patch shown in Fig. 1. L_6 and W_5 are significant parameters

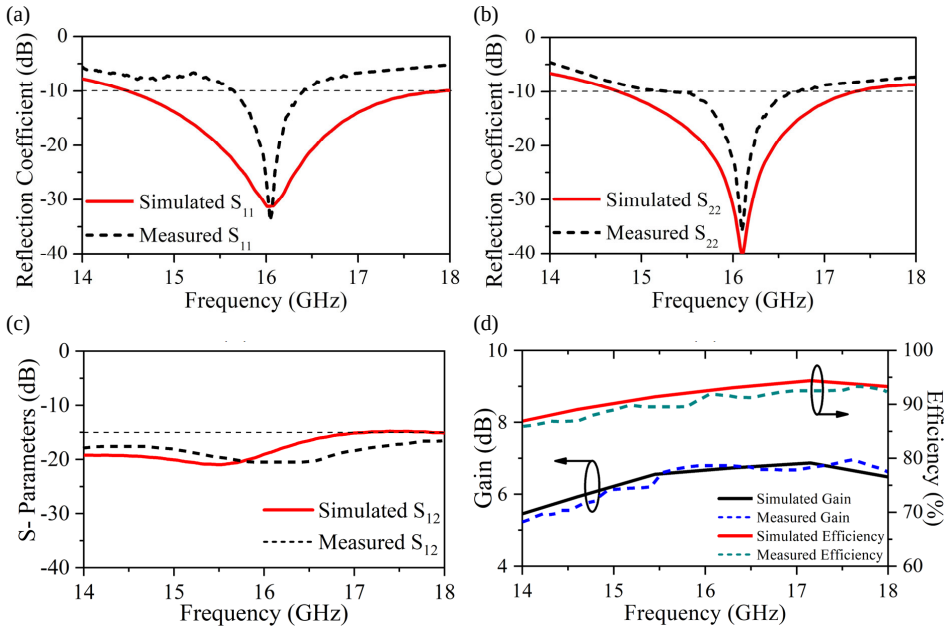

FIGURE 5. Simulated and measured (a) S_{11}, (b) S_{22}, (c) S_{12}, (d) gain and efficiency.

used for ground and microstrip feed line design, respectively. Fig. 4 shows the parametric analysis of different parameters.

Effect of the L-shaped slot: The effect of the L-shaped slot on the patch is calculated by varying the length parameters of slots L_3 and W_2 from 7 mm to 9 mm with a step size of 1 mm. When $L_3 = W_2 = 7$ mm, the reflection coefficient, bandwidth, and gain are lower than those of 8 mm. When $L_3 = W_2 = 9$ mm, bandwidth is slightly improved, but the reflection coefficient and gain are lower than those of 8 mm. Hence, the optimum values of L_3 and W_2 are 8 mm, as explained in Fig. 4(a). Similarly, the width parameters of the L-shaped slots L_2 and W_3 are changed from 0.5 mm to 1.5 mm with a linear step of 0.5 mm. When $L_2 = W_3 = 0.5$ mm and $L_2 = W_3 = 1.5$ mm, the two bandwidths remain the same. However, the reflection coefficients and gains of the antenna in these two cases are poor compared to $L_2 = W_3 = 1$ mm. Hence, the optimum values of L_2 and W_3 are 1 mm, as explained in Fig. 4(b).

Effect of the center rectangular slot: The length (L_4) and width (W_4) parameters of the rectangular slot on the patch are varied to know the impact of parameters on antenna characteristics. Parameter L_4 is varied from 3 mm to 5 mm with a linear step of 1 mm. When $L_4 = 3$ mm, 4 mm, and 5 mm, bandwidths of all three cases are the same. However, the gain and reflection coefficients are improved in the case of L_4 which is 4 mm. Hence, the optimum values of L_4 are considered to be 4 mm, as shown in Fig. 4(c). Similarly, parameter W_4 is changed from 5 mm to 7 mm with a step size of 1 mm. The bandwidth, reflection coefficient, and gain are enhanced in the case of $W_4 = 6$ mm compared to $W_4 = 5$ mm and 7 mm. Hence, the optimum value of W_4 is considered to be 6 mm, as explained in Fig. 4(d).

Effect of ground and feed line parameters: From the ground plane and microstrip feed line, parameters L_6 and W_5 are considered for analysis. Parameter L_6 is varied from 3 mm to 4 mm to 5 mm. When L_6 is 3 mm, there is no response within the band. When $L_6 = 5$ mm, again, bandwidth, reflection coefficient, and gain are less than those of 4 mm. Hence, the optimum value of L_6 is considered to be 4 mm, as explained in Fig. 4(e). Similarly, W_5 is another parameter from the feed line that is varied from 1 mm to 3 mm. When $W_5 = 1$ mm, 2 mm, and 3 mm, in all these cases, the bandwidths are almost the same. However, the remaining two antenna parameters are enhanced in the case of $W_5 = 2$ mm. Hence, the optimum value of W_5 is considered to be 2 mm, as explained in Fig. 4(f).

The transmission coefficient S_{12} and reflection coefficients S_{11} and S_{22}, and their simulated and measured values, along with the bandwidths and isolation, are shown in Figs. 5(a)–(c). According to Fig. 5(c), the CRSP antenna isolation between ports is below -15 dB. S_{21} is not depicted in Fig. 5(c) because of its identical configuration for brevity. The gain and efficiency of the CRSP antenna 2D plot are shown in Fig. 5(d).

3.3. MIMO Performance Metrics

The CRSP antenna parameters from [31, 33] are discussed and presented in Equations (4) to (15) in this section.

Envelope Correlation Coefficient (ECC): The value of the ECC can be obtained in two ways, one from S-parameters and the other from radiation patterns. The ECC value obtained from the far field is more accurate than S-parameters. Therefore, the ECC value obtained from the far-field radiation pattern is calculated using Equation (4).

$$\rho_e = \frac{\left|\iint_{4\pi}\left[F_{porti}\left(\theta,\varphi\right) * F_{portj}\left(\theta,\varphi\right)\right] d\Omega\right|^2}{\iint_{4\pi}\left|F_{porti}\left(\theta,\varphi\right)\right|^2 d\Omega \iint_{4\pi}\left|F_{portj}\left(\theta,\varphi\right)\right|^2 d\Omega} \tag{4}$$

The ideal value of ECC is zero. However, practically ECC $<$ 0.5 is accepted. The CRSP antenna with ECC $<$ 0.01 in the

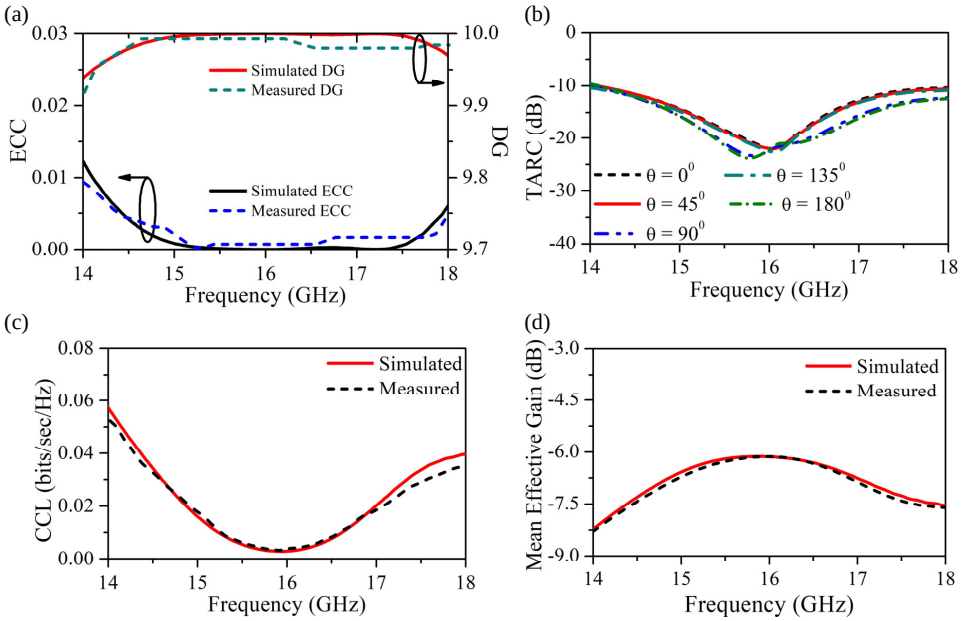

FIGURE 6. Simulated and measured (a) ECC and DG, (b) TARC, (c) CCL, (d) MEG.

entire band is presented in Fig. 6(a). At the resonant frequency of 16 GHz, the ECC value is almost zero.

Diversity Gain (DG): The DG of the proposed antenna can be obtained from ECC values using Equation (5).

$$\mathrm{DG} = 10\sqrt{1 - [\mathrm{ECC}]^2} \tag{5}$$

Fig. 6(a) explains the DG characteristics of the CRSP antenna. Ideally, the DG value is 10, and practically, a DG value of 9.99 is achieved for the CRSP antenna (close to the ideal value). Therefore, the CRSP antenna exhibits better diversity performance.

Total Active Reflection Coefficient (TARC): The total active reflection coefficient is defined as the ratio of reflected power to incident power. TARC for an N-port antenna can be calculated using Equation (6). The TARC values of the CRSP antenna at different angles are explained in Fig. 6(b).

$$\Gamma_a^t = \frac{\sqrt{\sum_{i=1}^{N} |b_i|^2}}{\sqrt{\sum_{i=1}^{N} |a_i|^2}}; \tag{6}$$

where a_i is the incident power, and b_i is the reflected power.

The scattering matrix for a 2×2 MIMO antenna can be described as

$$\begin{pmatrix} b_1 \\ b_2 \end{pmatrix} = \begin{pmatrix} S_{11} & S_{12} \\ S_{21} & S_{22} \end{pmatrix} \begin{pmatrix} a_1 \\ a_2 \end{pmatrix} \tag{7}$$

In a MIMO system, each excitation signal is randomly phased. Before arriving at the receiver, the propagation environment randomizes the signal phases once again.

$$b_1 = S_{11}a_1 + S_{12}a_2 = a_1\left(S_{11} + S_{12}e^{j\theta}\right) \tag{8}$$

$$b_2 = S_{21}a_1 + S_{22}a_2 = a_1\left(S_{21} + S_{22}e^{j\theta}\right) \tag{9}$$

Therefore, the TARC of 2×2 MIMO antenna is

$$\Gamma_a^t = \frac{\sqrt{\left|a_1\left(S_{11} + S_{12}e^{j\theta}\right)\right|^2 + \left|a_1\left(S_{21} + S_{22}e^{j\theta}\right)\right|^2}}{\sqrt{2\left|a_1\right|^2}} \tag{10}$$

The derivation of total active reflection coefficient (TARC) is presented in equation (10)

$$\Gamma_a^t = \frac{\sqrt{\left|\left(S_{11} + S_{12}e^{j\theta}\right)\right|^2 + \left|\left(S_{21} + S_{22}e^{j\theta}\right)\right|^2}}{\sqrt{2}} \tag{11}$$

Channel Capacity Loss (CCL): The channel capacity loss (CCL) of the CRSP antenna model is 0.04 bits/s/Hz within the band, as depicted in Fig. 6(c). The following equations are utilized to derive the measured channel capacity loss (CCL).

$$\mathrm{CCL} = -\log_2 \det\left(\psi^R\right); \tag{12}$$

where ψ^R is the Correlation matrix.

$$\psi^R = \begin{bmatrix} \phi_{11} & \phi_{12} \\ \phi_{21} & \phi_{22} \end{bmatrix} \tag{13}$$

where,

$$\begin{aligned} \phi_{ii} &= 1 - \left(|S_{ii}|^2 + |S_{ij}|^2\right) \\ \text{and } \phi_{ij} &= -\left(S_{ii}^* S_{ij} + S_{ji}^* S_{ij}\right) \end{aligned} \tag{14}$$

where i or $j = 1$ or 2 are the corresponding indices of S-parameters.

Mean Effective Gain (MEG): The mean effective gain of the MIMO antenna with "n" ports is obtained from S-parameters as shown in Equation (15).

$$\mathrm{MEG}_i = 0.5\left[1 - \sum_{j=1}^{n} |S_{ij}|^2\right]; \tag{15}$$

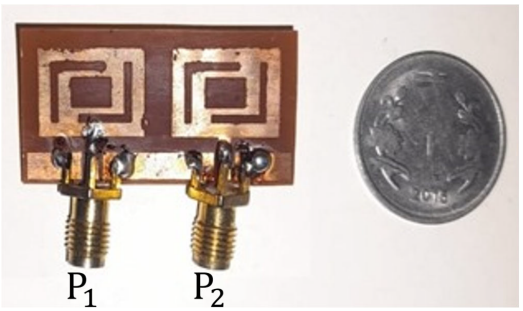

FIGURE 7. Fabricated prototype of CRSP antenna model.

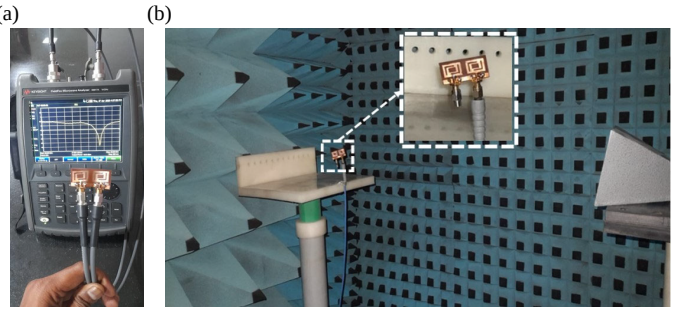

FIGURE 8. Measurement setup in anechoic chamber, (a) measurement calculations in VNA, (b) antenna under test setup.

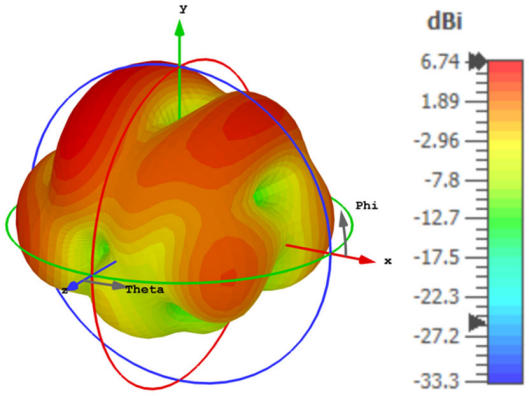

FIGURE 9. Gain plot of CRSP antenna at 16.0 GHz.

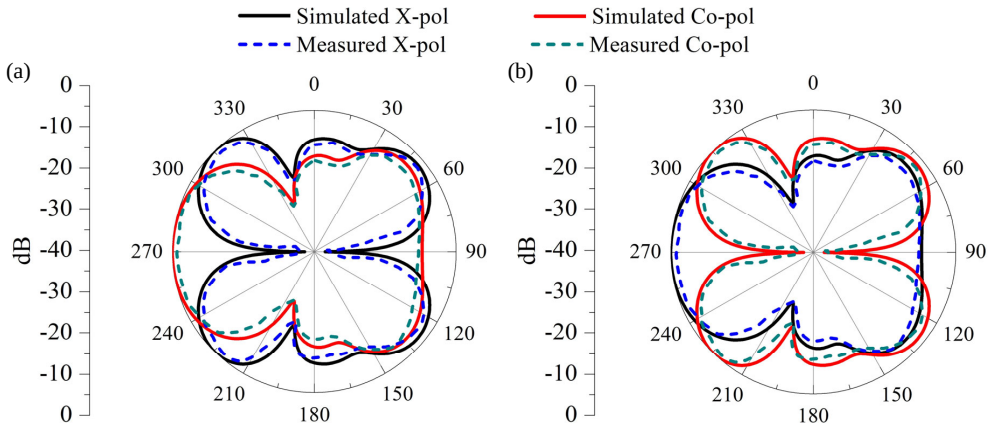

FIGURE 10. Radiation pattern of CSRP antenna at operating frequency (a) E-plane, (b) H-plane.

where i is the port number.

Ideally, MEG_i should be in the range of -3 dB to -12 dB (i.e., $-12\,\text{dB} < \text{MEG}_i < -3\,\text{dB}$). The CRSP antenna has MEG_i in between $-8\,\text{dB} < \text{MEG}_i < -6\,\text{dB}$, which is an accepted value to produce better diversity performance. Fig. 6(d) presents MEG_1 of the proposed two-port MIMO antenna for port 1. For port 2, MEG_2 is the same as MEG_1, with minute variations because of identical MIMO elements. Hence, MEG_2 is not displayed in Fig. 6(d) for brevity.

4. RESULTS AND DISCUSSIONS

The CST simulation software is used for designing and analyzing the single-band MIMO antenna. In a simulation, the antenna resonates with a -30 dB reflection coefficient at its operating frequency of 16.0 GHz. Also, a 2.8 GHz (14.6 GHz to 17.4 GHz) impedance bandwidth is observed. The prototype CRSP antenna model is fabricated to know the practical values of antenna parameters, and the measurement setup is depicted in Figs. 7 and 8(a), (b), respectively.

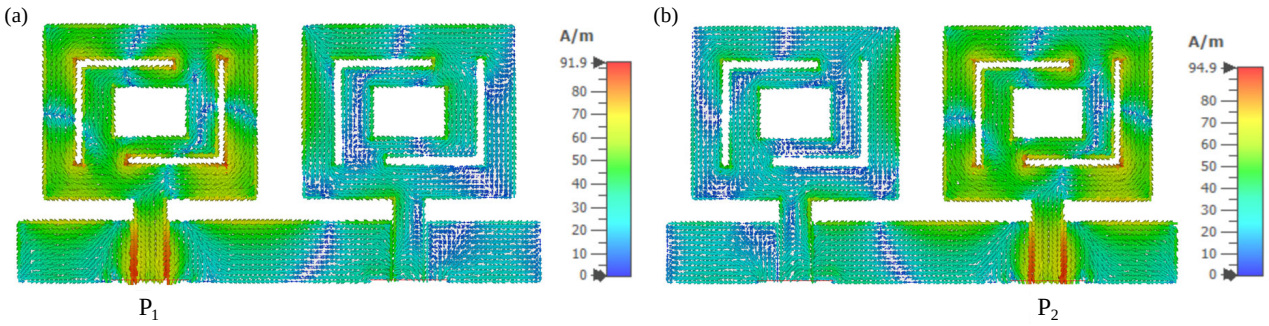

FIGURE 11. Surface current distribution of CRSP antenna, (a) port 1 (P_1) exited, (b) port 2 (P_2) exited.

TABLE 3. Comparison of CRSP antenna model with the existing models.

Ref. No	Antenna Size (mm^3)	Substrate Material	Resonating Frequency (GHz)	Gain (dBi)	Bandwidth (MHz)
[7]	$30 \times 30 \times 1.6$	FR-4	14.0	NA	1040
[8]	$50 \times 50 \times 1.52$	Epoxy glass FR4	15.9	1.55	1120
[9]	$50 \times 50 \times 1.52$	RF-35	13.9	3.73	920
[10]	$40 \times 40 \times 0.8$	FR-4	16.0	4.7	1000
[11]	$36 \times 36 \times 1.56$	Glass FR-4	16.0	1.59	1100
[Proposed CRSP antenna]	$20 \times 40 \times 0.07$	Kapton Polyimide	16.0	6.74	2800

NA — Not Available

The 3D gain plot of single-band MIMO antenna model is depicted in Fig. 9. From the plot, the CRSP antenna has a gain of 6.74 dBi over its operating frequency of 16.0 GHz. Figs. 10(a) and (b) show the antenna's simulated and measured radiation patterns of the co-polarization (Co-pol) and cross-polarization (X-pol) of the CRSP antenna with E and H planes. Figs. 11(a) and (b) show the surface current distribution at operational frequency. Also, this figure shows that the maximum currents of excitation at ports 1 and 2 are 91.9 A/m and 94.9 A/m, respectively. The highest current is seen where the rectangular patch feed line connects to the microstrip feed line. Table 3 compares the CRSP antenna with the most recent antenna models.

5. CONCLUSION

This paper provides an overview of a single-band, compact, two-port rectangle-shaped patch antenna with L-shaped and rectangle-shaped slots for wireless communication applications. The CRSP antenna is fabricated on a Kapton polyimide substrate of dimensions $20 \times 40 \times 0.07\,mm^3$. The CRSP antenna has an operating band of 14.6 GHz–17.4 GHz with an impedance bandwidth of 2.8 GHz. The isolation between the elements is greater than 15 dB. S-parameter characteristics, surface current distribution, radiation patterns, and MIMO parameters of the CRSP antenna are analyzed and presented in this paper. The proposed antenna operates at 16 GHz with a reflection coefficient of -30 dB. The CRSP antenna has ECC < 0.01, DG close to 10, and CCL < 0.04 bits/sec/Hz. A peak gain of 6.74 dBi is achieved at 16 GHz. The CRSP antenna has minimum isolation, low ECC, and good diversity performance. Therefore, it is proposed to be suitable for wireless communication applications.

ACKNOWLEDGEMENT

The fabrication of the antenna model work was supported by the Science and Engineering Research Board (SERB), DST, India, Grant no(s): EEQ/2016/000754; SB/FTP/ETA-0179/2014.

REFERENCES

[1] Kumar, R., G. S. Saini, and D. Singh, "Compact tri-band patch antenna for Ku band applications," *Progress In Electromagnetics Research C*, Vol. 103, 45–58, 2020.

[2] Saini, G. S. and R. Kumar, "A low profile patch antenna for Ku-band applications," *International Journal of Electronics Letters*, Vol. 9, No. 1, 47–57, 2021.

[3] Palla, R. and K. K. Naik, "Design of CPW fed E-shaped patch antenna with meandered slots for X-band applications," *International Journal of Microwave & Optical Technology*, Vol. 14, No. 2, 70–76, 2019.

[4] Hussain, M., M. A. Sufian, M. S. Alzaidi, S. I. Naqvi, N. Hussain, D. H. Elkamchouchi, M. F. A. Sree, and S. Y. A. Fatah, "Bandwidth and gain enhancement of a CPW antenna using frequency selective surface for UWB applications," *Micromachines*, Vol. 14, No. 3, 591, 2023.

[5] Nedil, M., M. A. Habib, T. Denidni, and H. Boutayeb, "Quasi-metallic-wall technique for increasing the efficiency of CB-CPW antennas," *Progress In Electromagnetics Research*, Vol. 78, 437–455, 2007.

[6] Krishna, O. R. and K. K. Naik, "Analysis of triangular antenna with two annular rings for multi-band applications," *Journal of Critical Reviews*, Vol. 7, No. 4, 189–191, 2020.

[7] Dahiya, A., R. Anand, N. Sindhwani, and D. Kumar, "A novel multi-band high-gain slotted fractal antenna using various substrates for X-band and Ku-band applications," *Mapan*, Vol. 37, No. 1, 175–183, 2022.

[8] Neet, N., R. Khanna, and J. Kaur, "Optimization of modified T-shape microstrip patch antenna using differential algorithm for X and Ku band applications," *Microwave and Optical Technology Letters*, Vol. 60, No. 1, 219–229, 2018.

[9] Nguyen Thi, T., K. C. Hwang, and H. B. Kim, "Dual-band circularly-polarised Spidron fractal microstrip patch antenna for Ku-band satellite communication applications," *Electronics Letters*, Vol. 49, No. 7, 444–445, 2013.

[10] Yalavarthi, U. D., "Reconfigurable orthogonal quad-port MIMO antenna for DSRC, WLAN, RADAR and Ku-band applications," *AEU — International Journal of Electronics and Communications*, Vol. 136, 153766, 2021.

[11] Phaneendra, C. N. and K. K. Naik, "Design of dual band MIMO antenna with rhombus shape for wireless applications," *Progress In Electromagnetics Research M*, Vol. 124, 63–70, 2024.

[12] Kumari, U. V. R., J. Srilakshmi, and K. K. Naik, "Exponential tapered patch antenna with DGS for C-band applications," in *2018 IEEE Indian Conference on Antennas and Propogation (InCAP)*, 1–3, IEEE, 2018.

[13] Ameen, M., A. Mishra, and R. K. Chaudhary, "Compact open-ended SIW antenna based on CRLH-TL and U-shaped slots for Ku-band application," *AEU — International Journal of Electronics and Communications*, Vol. 131, 153595, 2021.

[14] Lakrit, S., H. Ammor, J. Terhzaz, and A. Tribak, "Design of a new high-gain multiband and wideband rectangular patch antenna for C, X, and Ku band applications," *Walailak Journal of Science and Technology*, Vol. 14, No. 4, 339–351, 2017.

[15] Palla, R. and K. K. Naik, "Multiband rectangular microstrip patch antenna operating at C, X & Ku bands," in *2020 Third International Conference on Multimedia Processing, Communication & Information Technology (MPCIT)*, 19–25, 2020.

[16] Ye, Y., X. Zhao, and J. Wang, "Compact high-isolated MIMO antenna module with chip capacitive decoupler for 5G mobile terminals," *IEEE Antennas and Wireless Propagation Letters*, Vol. 21, No. 5, 928–932, 2022.

[17] Cheng, B. and Z. Du, "Dual polarization MIMO antenna for 5G mobile phone applications," *IEEE Transactions on Antennas and Propagation*, Vol. 69, No. 7, 4160–4165, 2021.

[18] Naik, K. K., R. K. Palla, S. S. Rani, and D. Gopi, "Design of S-band antenna with L-shaped slits on rectangular patch with defected ground structure," *International Journal of Measurement Technologies and Instrumentation Engineering*, Vol. 7, No. 2, 50–58, 2018.

[19] Wang, C., H. Wang, P. Wu, and M. Hou, "Dual-band closed-slot MIMO antenna for terminal wireless applications," *IEEE Transactions on Antennas and Propagation*, Vol. 70, No. 8, 6514–6525, 2022.

[20] Krishna, K. V., H. Khan, and K. K. Naik, "A compact rectangular shaped dipole array slot microstrip antenna with DGS for multi-band applications," *International Journal of Emerging Trends in Engineering Research*, Vol. 8, No. 2, 408–413, 2020.

[21] Hu, W., Z. Chen, L. Qian, L. Wen, Q. Luo, R. Xu, W. Jiang, and S. Gao, "Wideband back-cover antenna design using dual characteristic modes with high isolation for 5G MIMO smartphone," *IEEE Transactions on Antennas and Propagation*, Vol. 70, No. 7, 5254–5265, 2022.

[22] Sri, P. A. V. and K. K. Naik, "Analysis and design of trapezoidal shape CSRR rectangular patch antenna for wireless communications," *Microwave and Optical Technology Letters*, Vol. 65, No. 6, 1787–1793, 2023.

[23] Naik, K. K., M. Suman, and E. V. K. Rao, "Design of complementary split ring resonators on elliptical patch antenna with enhanced gain for terahertz applications," *Optik*, Vol. 243, 167434, 2021.

[24] Hussain, N., W. A. Awan, W. Ali, S. I. Naqvi, A. Zaidi, and T. T. Le, "Compact wideband patch antenna and its MIMO configuration for 28 GHz applications," *AEU — International Journal of Electronics and Communications*, Vol. 132, 153612, 2021.

[25] Naik, K. K., B. V. Krishna, G. Srikanth, L. V. Kumar, B. V. Priya, and P. A. V. Sri, "Compact circular patch with meander line monopole antenna for X-band applications," in *Proceedings of the International Conference on Electronics, Communication and Aerospace Technology, ICECA*, 454–458, Apr. 2017.

[26] Chattha, H. T., M. K. Ishfaq, B. A. Khawaja, A. Sharif, and N. Sheriff, "Compact multiport MIMO antenna system for 5G IoT and cellular handheld applications," *IEEE Antennas and Wireless Propagation Letters*, Vol. 20, No. 11, 2136–2140, 2021.

[27] Sri, P. A. V., N. Yasasvini, M. Anjum, A. V. Manikanta, D. N. S. S. Harsha, G. Dattatreya, and K. K. Naik, "Analysis of wideband circular ring with rectangular patch antenna for airborne radar application," in *Proceedings of the International Conference on Electronics, Communication and Aerospace Technology, ICECA*, 459–461, Apr. 2017.

[28] Recioui, A. and H. Bentarzi, "Genetic algorithm based MIMO capacity enhancement in spatially correlated channels including mutual coupling," *Wireless Personal Communications*, Vol. 63, No. 3, 689–701, 2012.

[29] Recioui, A., "Capacity optimization of MIMO systems involving conformal antenna arrays using a search group algorithm," *Algerian Journal of Signals and Systems*, Vol. 5, No. 4, 209–214, Dec. 2020.

[30] Naik, K. K. and M. H. V. Manikanta, "Design of circular slot on rectangular patch with meander line antenna for satellite communications," in *Proceedings of the International Conference on Inventive Communication and Computational Technologies, ICICCT*, 1252–1255, Apr. 2018.

[31] Sufian, M. A., N. Hussain, A. Abbas, J. Lee, S. G. Park, and N. Kim, "Mutual coupling reduction of a circularly polarized MIMO antenna using parasitic elements and DGS for V2X communications," *IEEE Access*, Vol. 10, 56 388–56 400, 2022.

[32] Abbas, A., N. Hussain, M. A. Sufian, W. A. Awan, J. Jung, S. M. Lee, and N. Kim, "Highly selective multiple-notched UWB-MIMO antenna with low correlation using an innovative parasitic decoupling structure," *Engineering Science and Technology, An International Journal*, Vol. 43, 101440, 2023.

[33] Ahmad, S., S. Khan, B. Manzoor, M. Soruri, M. Alibakhshikenari, M. Dalarsson, and F. Falcone, "A compact CPW-fed ultra-wideband multi-input-multi-output (MIMO) antenna for wireless communication networks," *IEEE Access*, Vol. 10, 25 278–25 289, 2022.